Computation of Relative Bond Dissociation Enthalpies (ΔBDE) of Phenolic Antioxidants from Quantum Topological Molecular Similarity (QTMS)

Nakul Singh, Robert J. Loader, Patrick J. O'Malley, and Paul L. A. Popelier*

School of Chemistry, Sackville Street, The University of Manchester, Manchester, M60 1QD, U.K.

Received: September 22, 2005; In Final Form: March 8, 2006

A recently proposed method called quantitative topological molecular similarity (QTMS) generated a model for the computation of the relative substituent effects on the bond dissociation enthalpies (ΔBDEs) for a set of 39 phenols. The data set includes a diverse set of substituents with monosubstituted and poly-substituted derivatives that exhibit different electronic and steric effects. Many share common structural features with already well-established antioxidants. QTMS reveals the active region of the substituted phenols and identifies the electronic descriptors that best explain the range of ΔBDEs observed. For substituents in the 4-X position (para) we find that our model requires a correction for radical stabilization enthalpy (RSE). Application of the QTMS methodology yields an unrivalled QSAR with $r^2 = 0.98$ and $q^2 = 0.85$ for the bond dissociation enthalpies of this phenolic antioxidant data set.

Introduction

The degradation of carbon-based materials (RH) is usually caused by peroxyl radical initiation (eq 1) followed by a chemical reaction with molecular oxygen to generate more peroxyl radicals (eq 2). This process, known as autoxidation, can propagate and generate more peroxide and free radicals.

Chain Propagation

$$ROO^{\bullet} + RH \rightarrow ROOH + R^{\bullet} \quad (1)$$

$$R^{\bullet} + O_2 \rightarrow ROO^{\bullet} \quad (2)$$

It is well-known that phenols can operate as chain-breaking and peroxyl radical-trapping antioxidants, which inhibit the peroxidation of carbon based materials. The study of phenolic antioxidants has generated much attention in recent years, due to their use in the pharmaceutical and chemical industry.[1] The phenol donates a hydrogen atom and in the process terminates the propagation of further radical reactions as outlined in eqs 3 and 4.

Chain Termination

$$ArOH + ROO^{\bullet} \rightarrow ArO^{\bullet} + ROOH \quad (3)$$

$$ArO^{\bullet} + ROO^{\bullet} \rightarrow \text{nonradical products} \quad (4)$$

The role of an antioxidant is to intercept a free radical before it can react with a substrate[2]. The rate constant for the H atom transfer (eq 3) must be much higher than the rate constant for eq 1, i.e., $k_3 \gg k_1$. For antioxidant activity, the derived radical ($ArO^{\bullet}$) after hydrogen abstraction should be stable, eventually decomposing to nonradical products.

Developments in computational power and progress in quantum chemical calculations, particularly in density functional theory (DFT), are making the study of these reactions easier.[3−5] Ideally, we would calculate the activation energy for eq 3 since it is the rate constant that determines the outcome. Theoretical analysis of model systems of eq 3 lead to a deeper understanding of the mechanism than can be obtained by experiment. The former provides access to details of the underlying mechanism that are not available from the latter.[6] However, because of the approximations in the calculations, where possible, it is important to compare theoretical results with experimental results. Recent studies using variational transition state theory showed that theoretical rate constants of the reaction of α-tocopherol with hydroperoxyl showed good agreement with available experimental rate constants results.[7,8] In contrast to employing transition state theory to determine the rate constants, thermochemistry provides a useful look at the problem and is computationally much less demanding.

Quantum thermochemical calculation of the O−H bond dissociation enthalpy (BDE) is known to be successful for characterizing antioxidant activity for a large number of antioxidants.[9,10] There are many experimental methods developed for the determination of the O−H bond dissociation enthalpy (BDE) of phenols. Quantum calculations of the bond dissociation enthalpies can reproduce experimental BDEs to a good chemical accuracy.[9] Substituent additivity scales based on the relative bond dissociation enthalpies to phenol (ΔBDE) show that electron donating groups introduced on the phenol ring enhance the antioxidant activity. However, there are cases where quantum thermochemical calculations are poor, especially when steric and intramolecular interactions occur.[9]

One other method to determine the ΔBDEs of phenols is based on quantitative structure activity/property relationships (QSAR/QSPR). Many authors have attempted to elucidate the QSAR of phenolic antioxidants by using a plethora of different descriptors. QSARs based on energy parameters such as ionization potential, proton dissociation energies and highest occupied molecular orbital energies have been reported.[11,12] Others have used structural based descriptors such as the number of hydroxyl groups, topographic electronic index, ZX shadow etc.[13−15] Finally, there are some QSARs based on interpreting the electron density featuring comparative molecular field analysis CoMFA.[16] Recent CoMFA analysis utilizes the 3D grid

* Corresponding author. E-mail: pla@manchester.ac.uk. Telephone: +44-161-3064511. Fax: +44-161-3064559.

10.1021/jp0553885 CCC: $33.50
Published on Web 04/28/2006

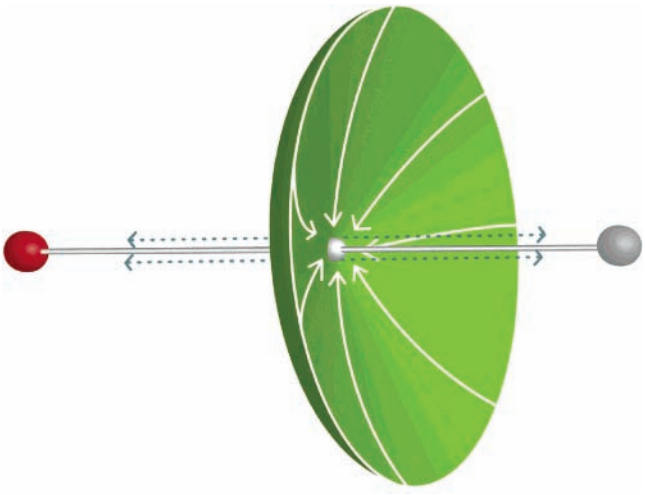

Figure 1. Representation of the electron density (ρ) at the BCP. The arrows show the direction of increasing ρ. The BCP is a special point called a saddle point. It appears at a minimum in the electron density on the axis lying between the associated nuclei and at a maximum in the plane perpendicular to this.

superposition of electron density to highlight the active site around the lone pair oxygen and around the 4-X (or para) substituent.[17] The CoMFA analysis shows that a decrease in electron density around the lone pair of the oxygen atom, in conjunction with an increasing electron density at substituents on the 4-X position, correlates with a weakening of the O−H bond. Most, if not all the QSAR work reviewed here employ semiempirical methods.

In this study, we employ a computational technique called quantum topological molecular similarity (QTMS), which makes use of electron density analysis of the wave function of optimized phenols.[18] The approach we use correlates bond critical point properties (BCPs) with the ΔBDEs of 39 phenols taken from Bordwell et al.,[19] as measured in DMSO. QTMS[20] has been applied before in a wide variety of activities and properties, such as antitumor activity of phenylbutenones,[21] mutagenicity of furanones and triazenes,[22] steroid binding affinity and antibacterial activity of nitrofuran derivatives,[23] activity of 1,4-dihydropyridine calcium channel blockers,[24] pK_a of phenols, anilines and carboxylic acids,[25] computation of ester hydrolysis rate constants,[26] and toxicity of polychlorinated dibenzo-*p*-dioxins (PCDDs).[27] It was also proven that QTMS can substitute for the appropriate Hammett constants.[28]

Computational Method

To understand the QTMS technique, one must envision the molecule as a collection of atomic "attractors" (nuclei) surrounded by a sea of charge density. Between each pair of bonded atoms there exists a pathway of charge density called a bond path. Somewhere along this path there is a minimum point of electron density in the plane of the bond path, but a maximum in the plane perpendicular commonly known as a saddle point.[29,30] This saddle point is called a BCP and is illustrated in Figure 1.

Properties are evaluated at each BCP for each of the molecules in the data set that share a common molecular skeleton, see Figure 2. A multilinear regression technique called partial least squares (PLS) is then performed in order to derive a relationship between the BDE and the BCP properties.

Initially we used the semiempirical AM1 method to optimize all the phenols in this study and generate the wave functions. In accord with our other QTMS work this is referred to as level

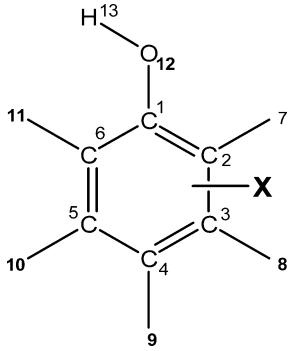

Figure 2. Common molecular skeleton for the phenol data set.

A,[31] while level B refers to HF/6-31G(d)//HF/6-31G(d). This standard notation of Gaussian basis sets describes a geometry optimization at the Hartree−Fock level using the 6-31G(d) basis set followed by the wave function calculation at this same level. Finally, for level C calculations, we employ the B3LYP hybrid DFT method, with the 6-31+G(d,p) basis set. All geometry optimizations were carried out with GAUSSIAN03W suite of programs.[32] The wave functions obtained at levels A−C are read in by a local version of MORPHY98, which locates the BCP and evaluates all the topological properties required for this study.[33]

When modeling BCP properties we have 4*N* variables (X) where *N* is the number of bonds. The PLS method is implemented using SIMCA-P[34] and is used to find a relationship between the observed *Y* variables (BDEs) and the *X* variables (AIM descriptors and bond lengths). The PLS model[35] is able to manage a large number of *X* variables, and can handle noise, collinear and even multilinear variables.[36] As a supervised method PLS combines linear least-squares with principal component analysis and constructs linear combinations of the *X*-variables, called latent variables (LV). For AM1 level of theory, unreliable topologies are produced in that BCPs may not be present due to the absence of core orbitals.[37] In general BCP properties cannot be used in conjunction with semiempirical methods without explicit and artificial addition of core densities a posteriori. Therefore, we only use bond lengths as our X variables at this level. At the higher levels of theory where AIM descriptors are better defined, we use four components all evaluated at the BCP ($\rho(r)$, $\nabla^2\rho(r)$, ϵ, $K(\mathbf{r})$). The first descriptor is the electron density $\rho(r)$. The Laplacian of the charge density, the quantity $\nabla^2\rho$, has the important property of determining where electronic charge is locally concentrated ($\nabla^2\rho(r) < 0$) and locally depleted ($\nabla^2\rho(r) > 0$). The ellipticity, ϵ, of a bond is one measure of its π character, as determined by the extent to which charge is preferentially accumulated in a given plane. It is defined as $\lambda_1/\lambda_2 - 1$ where $\lambda_1 < \lambda_2 < 0$ are the two negative eigenvalues of the Hessian[30] at the BCP. The final AIM descriptor we consider is a type of local kinetic energy density $K(\mathbf{r})$. This density, denoted by K(**r**), is defined as $K(\mathbf{r}) = -{}^1/_4 N \int d\tau' [\psi^*\nabla^2\psi + \psi\nabla^2\psi^*]$, where ψ is the many-electron wave function and $\int d\tau'$ denotes an integration over the spin coordinates of all *N* electrons except one. Interpreting K(**r**) in chemical terms is not straightforward although useful formulas describing its link to the Laplacian and the more "classical" kinetic energy G(**r**) can be found elsewhere.[38]

After constructing the matrix of descriptors we perform a partial least-squares analysis with these *X* variables and the activities, *Y*, which in this case is the BDE values of the phenols taken from Bordwell et al.[19] The quality of the models is assessed by several regression statistics. (i) The r^2 correlation coefficient measures the quality of the fit produced. (ii) The

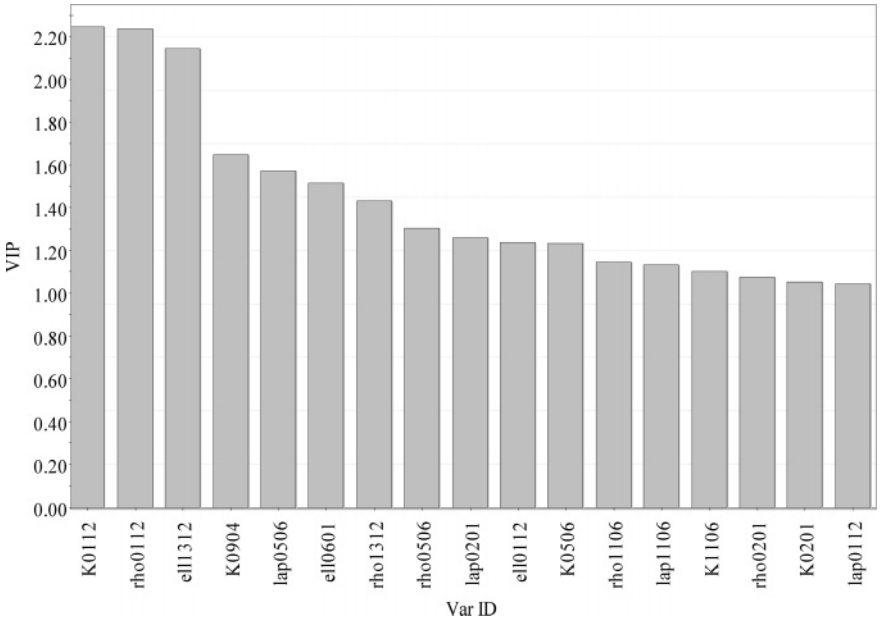

Figure 3. VIP plot for all phenols from the PLS analysis calculated at level C. The abbreviations *K*, rho, ell, and *lap* refer to the kinetic energy density, the electron density, the ellipticity, and the Laplacian of the electron density, respectively. The location of the bond is marked by four digits that should be read as two consecutive pairs, each pair referring to an atomic label in Figure 2.

q^2, also known as the cross-validated r^2, measures the internal predictivity, based on SIMCA-P's default "leave one-seventh of the data out" rather than the "leave one out", which is thought to be problematic.[39] Note that q^2 is an estimate of the predictive ability of the model, and calculated by cross-validation. The data are divided into 7 parts (by default) and each one-seventh removed in turn. A model is built on the six-seventh data left in, while the left-out data are predicted from the new model. This is repeated with each one-seventh of the data until all the data have been predicted. The predicted data are then compared with the original data and the sum of squared errors calculated for the whole data set. This is then called the predicted residual sum of squares (PRESS).[36] The better the predictability of the model, the lower this value will be. For convenience one converts the PRESS into q^2 to resemble the scale of the r^2. (iii) The overall quality of the model is assessed by r^2(int) and q^2(int); to safeguard against correlations determined by chance these two statistics are calculated via a randomization validation test. The test estimates the probability that a good fit will be obtained after random reorganization of the dependent variables. That is, the wrong activity is associated with the wrong electronic descriptors. Each r^2 and q^2 generated is then plotted against the absolute value of the correlation coefficient between the original set of activities and its permutation. Lines are drawn through the r^2 and q^2 values and the intercepts examined. A model is deemed valid if the r^2(int) < 0.4 and q^2(int) < 0.05. The randomization test must be performed at least 10 times to ensure that a good model is not merely the result of pure chance. Together these statistical measures provide a rigorous framework to assess the quality of the models constructed. We do not explicitly report these statistics but guarantee that all models passed this validation test.

To detect the active center we use SIMCA-P's variable importance plot (VIP). A VIP value above 1 for any variable is deemed significant to the model and anything below 1 is regarded as unimportant.[35] There are no rigorous statistical criteria to determine the active site but in some cases the data lends itself to detecting it easily, as we see below.

Results and Discussion

The variable importance plot (VIP) plot, for the level C BCP model implicates two bonds, C_1-O_{12} and $O_{12}-H_{13}$ as the most significant in the model, as shown in Figure 3.

The electron density and kinetic energy descriptors at the BCP of C_1-O_{12} are the most important followed by the ellipticity descriptor at the $O_{12}-H_{13}$ bond. Although we do not show the VIP plots for other levels, they share almost identical trends with that of level C. We see in the VIP plots a sharp drop off after the first three descriptors. This indicates that the active site is centered mainly near the C_1-O_{12} bond and extends through to the ellipticity (ϵ) of the $O_{12}-H_{13}$ bond. One would expect with chemical intuition that the active site will be directly centered on the O−H bond but this is not the case. The BDE model is affected by the stabilization of the phenols due to delocalization of the lone pair on the oxygen by 4-X substituted phenols.[19] This delocalization of lone pair electrons is likely to be most prominent on the C_1-O_{12} bond. The kinetic energy descriptor associated with this bond, denoted by K0112, shows an extremely collinear relationship with the rho0112 parameter at the active site, as shown in Figure 4.

There is strong evidence linking the bond order of C−O bonds with the Kinetic energy descriptor at the bond critical point, suggesting that the bond order may be an appropriate descriptor in characterizing the activity of antioxidants.[40] For all intents we discard the K0112 parameter because of the redundancy in information it shares with the rho0112 values. Theoretical studies indicate that increasing the electron density in the $O_{12}-H_{13}$ bonding region correlates with an increase in the bond strength. Recent work has confirmed this to be true,[41] however, no direct relationship can be found between the rho1213 and the O−H bond strengths of phenols.[41] Our work is in overall agreement because we do not find the rho1213 to be important in the model, as it appears only in the seventh position.

There are some outliers, all of which occupy the 4-X position; see Figure 5 and Table 1. The electron donors 4-NH_2, 4-NMe_2, 4-OMe, and 4-Ph are poorly fitted by our equation, and it is of interest to understand why this is so. Similarly three electron

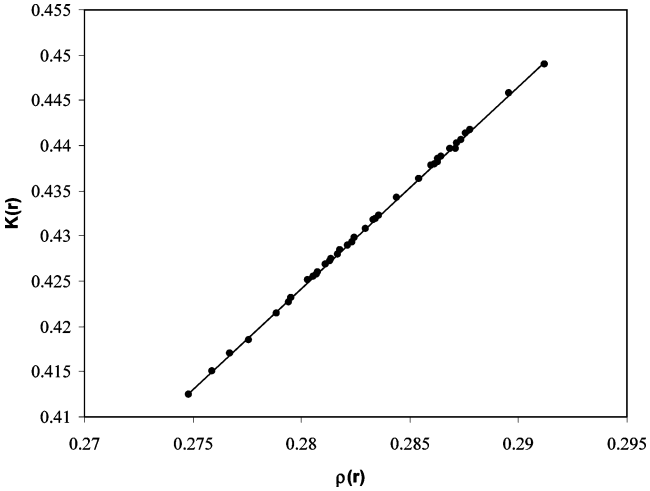

Figure 4. Plot of the kinetic energy density, K(**r**), vs electron density, ρ, at the C_1-O_{12} bond critical point calculated at level C.

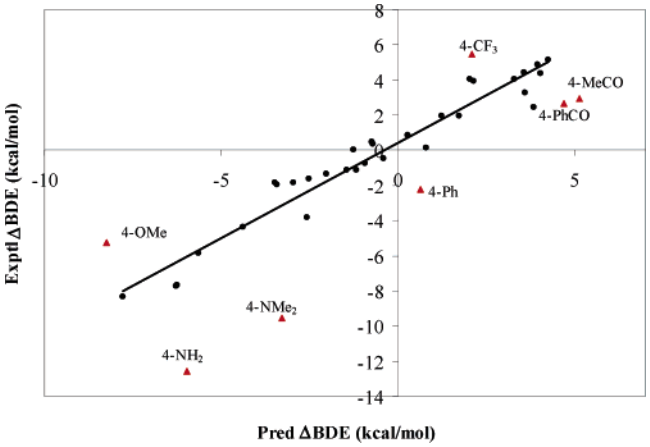

Figure 5. Plot of experimental ΔBDE values vs computed ones, calculated at level C. The outliers are marked with triangles and substituent name. The 4-O^- substituent is not shown here.

withdrawing groups, 4-CF_3, 4-MeCO, and 4-PhCO, are found also to be outliers.

Radical stability has usually been equated to the bond dissociation enthalpy. However, in this case the bond dissociation enthalpy is the difference in the heat of formation of the radical and the initial parent molecule, and therefore it cannot solely be attribute to only electronic effects. Dust and Arnold advocated[42] the use of a dual Hammett parameter relationship for radical reactions:

$$\Delta\mathrm{BDE} = \rho\sigma^{+} + \rho\sigma\bullet \qquad (5)$$

We have demonstrated before that the QTMS procedure offers a good substitute for Hammett substituent constants,[28] and therefore, the first part of the equation is well accounted for in this study. However, the component energy due to the delocalization of the spin density is not taken into account in this work. We can compute this energy by subtracting the observed value from the predicted

$$\Delta\mathrm{RSE} = \Delta\mathrm{BDE}_{\mathrm{obs}} - \Delta\mathrm{BDE}_{\mathrm{pred}} \qquad (6)$$

where RSE are the radical stabilization enthalpies.

Other authors[41,43,44] have also estimated ΔRSE values, each of which obtained by different procedures, occasionally involving large differences. Their values and our own, based on eq 6, are listed in Table 2. It appears that lone pair delocalization dominates over delocalization for all substituents except those in the 4-X position. ΔRSE is expected to feature strongly for

TABLE 1: Observed vs Computed ΔBDE[a] Values (kcal/mol) Calculated at Level C

substituent (X)	exptl ΔBDE (kcal/mol)	pred ΔBDE (kcal/mol)
H	0	−1.24
2-Me	−1.65	−2.51
3-Me	−0.45	−0.4
4-Me	−1.15	−1.45
3,5-Me_2	−0.75	−0.92
2,6-Me_2	−4.35	−4.39
4-*t*-Bu	−1.15	−1.17
2,6-*t*-Bu_2	−7.75	−6.26
2,4,6-*t*-Bu_3	−7.65	−6.26
4-Ph[b]	−2.25	0.63
2-MeO	−3.85	−2.58
3-MeO	0.35	−0.7
4-OH	−8.35	−7.78
3-NH_2	−1.85	−3.49
3-Me_2N	−1.95	−3.41
4-NH_2[b]	−12.55	−5.96
4-NMe_2[b]	−9.55	−3.28
2-Cl	0.15	0.79
3-Cl	1.95	1.74
4-Cl	0.45	−0.73
3,5-Cl_2	4.05	3.29
3,4,5-Cl_3	3.25	3.6
4-Br	0.85	0.27
3-CF_3	3.95	2.14
4-CF_3[b]	5.45	2.09
3-MeCO	1.95	1.23
4-MeCO[b]	2.95	5.13
3-NO_2	4.45	3.57
4-NO_2	4.85	3.97
4-OMe[b]	−5.25	−8.25
4-PhCO[b]	2.65	4.7
3-$MeSO_2$	2.45	3.85
4-$MeSO_2$	5.15	4.26
3-CN	4.05	2.03
4-CN	4.35	4.05
1-NpOH	−5.85	−5.65
4-O^-	−16.85	−19.02
2-NpOH	−1.85	−2.95
6-Br-2-NpOH	−1.35	−2.03

[a] ΔBDE = BDE(X-phenol) − BDE(phenol); Np = naphthol. [b] Outliers in the model.

TABLE 2: Computed ΔBDE Values Corrected with Radical Stabilization Enthalpies[a]

substituent (X)	ΔRSE[b]	ΔRSE[c]	ΔRSE[d]	ΔBDE[e]	ΔRSE[f]
4-NMe_2	*−8.2*	*−8.1*	*−6.9*	*−3.3*	*−6.3*
4-NH_2	*−7.2*	*−7.6*	*−8.8*	*−6.0*	*−6.6*
4-OMe	***−4.4***	***−4.3***	***−3.4***	***−8.3***	***3.0***
4-Ph			*−3.1*	*0.6*	*−2.9*
4-OH	**−4.1**	**−3.8**	**−5.5**	**−7.8**	**−0.6**
4-Me	−1.7	−2.3	0.2	−1.5	0.3
4-Cl	−1.8		−0.7	−0.7	1.2
4-Br			−0.9	0.3	0.6
4-*t*-Bu			0	−1.2	0
4-MeCO	-	-	*−1.5*	*5.1*	*−2.1*
4-PhCO	-	-	*−2.6*	*4.7*	*−2.0*
4-CN	−2.1	1.4	−0.8	4.1	0.3
4-CF_3	*0.8*	*2.6*	*1.9*	*2.1*	*3.4*
4-NO_2	0.1	3.1	−5.8	4.0	0.9
4-$MeSO_2$				4.3	0.9
4-O^-				−19.0	−2.2

[a] Values in italics refer to the seven outliers identified in Figure 5. The bold values refer to phenols showing a discrepancy of more than 2 kcal/mol with any of the alternative ΔRSE values (columns 2, 3 and 4). [b] Values taken from ref 41. [c] Values taken from ref 43. [d] Values taken from ref 44. [e] Predicted by our model (see Table 1). [f] This work, from eq 6.

TABLE 3: PLS Statistics for ΔBDE Models Using the Pruned[a] Phenol Data Set

model	level of calculation	descriptors	LVs[b]	r^2	q^2
1	level B	BCP properties	4	0.96	0.76
2	level C	BCP properties	4	0.98	0.85
3	level A	bond lengths	2	0.86	0.61
4	level B	bond lengths	2	0.82	0.55
5	level C	bond lengths	2	0.82	0.51

[a] Seven outliers, marked by triangles in Figure 5 have been taken out. [b] Number of latent variables.

such compounds. This is why we calculated the ΔRSE values of all 16 4-X phenols in this study and compared them to three alternative values. Only two substituents (4-OMe and 4-OH) show a discrepancy of more than 2 kcal/mol between the current ΔRSE values and any of the three alternative ΔRSE values. Discarding these, the average mean absolute error amounts to 0.6 kcal/mol.

Despite the appearance of two outliers, the QSAR is able to correctly reproduce the Δ*B*DE values of sterically hindered phenols (2,6-*t*-Bu_2 and 2,4,6-*t*-Bu_3), which are related to industrially important phenols. It is worth mentioning that a (RO)B3LYP/6-311+G(2d,2p)//AM1/AM1 calculation[9] on 2,6-*t*-Bu_2 in the gas phase (76.5 kcal/mol) yielded a discrepancy with experiment (82.8 kcal/mol) amounting to about four times our discrepancy (1.5 kcal/mol). It should be recognized that the QSAR has been trained to relate Δ*B*DEs measured in DMSO to structural and topological features of gas phase molecules, admittedly computed at lower level. Solvent effects do play a role in determining[44] absolute BDEs. Hydrogen bonds to hindered phenols can change the dihedral angle between the OH group and the aromatic plane, and thereby influence the BDE. For example, a recent study[45] combining ^{1}H NMR and medium level ab initio calculations on a complex of 2,6-di-*tert*-butyl-4-methylphenol (BHT) and carboxylic acid esters confirmed this effect. To the best of our knowledge no ab initio calculations have taken into account solvent effects on the BDE of sterically hindered phenols, However, computational studies[46,47] on nonhindered phenols show that hydrogen-bond forming solvents increase the BDE. One might expect similar PCM or semicontinuum models to raise the BDE of 2,6-*t*-Bu_2 as well (above 76.5 kcal/mol), thereby reducing the discrepancy with experiment.

The AM1 bond lengths produce models that, surprisingly, deteriorate in quality when using higher level calculations; see Table 3. However, all bond length models identify the C_1-O_{12} bond as the most important descriptor. The observation that level A bond lengths perform better than the higher levels B and C can be rationalized by comparing experimental C_1-O_{12} bond lengths to those calculated here. We find that the reported experimental C_1-O_{12} phenol (1.375 Å) bond lengths are at level A (1.377 Å), level B(1.353 Å), and level C (1.372 Å). The AM1 C_1-O_{12} bond length is the closest to the experimental value indicating that the AM1 geometry optimization may be adequate for the geometry optimization of phenols.[48]

The models constructed from BCP properties are superior to the bond length models with greatly improved statistics. The best model is obtained at level C ($r^2 = 0.98$, $q^2 = 0.85$). One must consider that level C is adequate in terms of results. It is common now to define how good a QSAR model is by comparing the r^2 and q^2 statistics. On this basis these results are excellent and improve upon other reported models.[14]

Conclusions

Because of ever increasing computing power, it is now possible to construct models for a variety of properties, such as bond dissociation enthalpies, using descriptors drawn from realistic wave functions. A rigorous statistical treatment permits the extraction of important features that best describe the activity being modeled. In analyzing the common skeleton, we successfully use the QTMS method to highlight the most important bonds that are responsible for the ΔBDE. The C_1-O_{12} bond is selected as the most important bond represented by the VIP plots for both the bond length and BCP models. We find that radical stabilization is important for 4-X substituents and propose that any future models should include this correction factor. Increasing the level of theory significantly improves our model, with the best being achieved at a modest B3LYP/6-31+G(d,p) level of theory.

Acknowledgment. We thank the EPSRC for their financial support, group members Michel Rafat and Michael Devereux, and Arjun Singh for their help in preparing Figure 1.

References and Notes

(1) Rice-Evans, C. A.; Miller, N. J.; Paganga, G. *Free Radical Biol. Med.* **1996**, *20*, 933.
(2) Burton, G. W.; Doba, T.; Gabe, E. J.; Hughes, L.; Lee, F. L.; Prasad, L.; Ingold, K. U. *J. Am. Chem. Soc.* **1985**, *107*, 7053.
(3) Espinosa-Garcia, J. *Chem. Phys. Lett.* **2004**, *388*, 274.
(4) O'Malley, P. J. *J. Phys. Chem. B* **2002**, *106*, 12331.
(5) O'Malley, P. J. *Chem. Phys. Lett.* **2002**, *364*, 318.
(6) Singh, N.; O'Malley, P. J.; Popelier, P. L. A. *Phys. Chem. Chem. Phys.* **2005**, 614.
(7) Navarette, M.; Rangel, C.; Espinosa-Garcia, J.; Corchado, J. C. *J. Chem. Theor. Comput.* **2005**, *1*, 337.
(8) Viloca-Garcia, M.; Gao, J.; Karplus, M.; Truhlar, D. G. *Science* **2004**, *303*, 186.
(9) Wright, J. S.; Johnson, E. R.; DiLabio, G. A. *J. Am. Chem. Soc.* **2001**, *123*, 1173.
(10) Wright, J. S. *Chem. Br.* **2003**, *February*, 25.
(11) Van Acker, S. A. B. E.; Koymans, L. M. H.; Bast, A. *Free Radical Biol. Med.* **1993**, *15*, 311.
(12) Zhang, H.; Sun, Y.; Wang, X. *J. Org. Chem.* **2002**, *67*, 2709.
(13) Lien, E. J.; Ren, S.; Bui, H.; Wang, R. *Free Radical Biol. Med.* **1999**, *26*, 285.
(14) Bosque, R.; Sales, J. *J. Chem. Inf. Comput. Sci.* **2003**, *43*, 637.
(15) Zhang, H. Y.; Sun, Y. M.; Zhang, G. Q.; Chen, D. Z. *Quant. Struct. Act. Relat.* **2000**, *19*, 375.
(16) Yamagami, C.; Akamatsu, M.; Motohashi, N.; Hamada, S.; Tanahashi, T. *Biorg. Med. Chem. Lett.* **2005**, *15*, 2845.
(17) Vaz, R. J.; Edwards, M.; Shen, J.; Pearlstein, R.; Kominos, D. *Int. J. Quantum Chem.* **1999**, *75*, 187.
(18) O'Brien, S. E.; Popelier, P. L. A. *J. Chem. Inf. Comput.Sc.* **2001**, *41*, 764.
(19) Bordwell, F. G.; Cheng, J.-P. *J. Am. Chem. Soc.* **1991**, *113*, 1736.
(20) Popelier, P. L. A. Quantum topological molecular similarity—past, present and future. In *EuroQSAR 2002: Designing Drugs and Crop Protectants: processes, problems and solutions*; Ford, M., Livingstone, D. J., Dearden, J., van de Waterbeemd, H., Eds.; Blackwell: Blackwell, Oxford, G.B., 2003; p 130.
(21) O'Brien, S. E.; Popelier, P. L. A. *J. Chem. Soc., Perkin Trans. 2* **2002**, 478.
(22) Popelier, P. L. A.; Chaudry, U. A.; Smith, P. J. *J. Comput.-Aided Mol. Design* **2004**, *18*, 709.
(23) Smith, P. J.; Popelier, P. L. A. *J. of Comput.-Aided Mol.Design* **2004**, *18*, 135.
(24) Chaudry, U. A.; Singh, N.; Popelier, P. L. A. *A Quantitative Structure−Activity Relationship of 1,4-Dihydropyridine Calcium Channel Blockers with Electronic Descriptors produced by Quantum Chemical Topology*; Labbe, A. T., Ed.; Kluwer: Dordrecht, The Netherlands, 2006.
(25) Chaudry, U. A.; Popelier, P. L. A. *J. Org. Chem.* **2004**, *69*, 233.
(26) Chaudry, U. A.; Popelier, P. L. A. *J. Phys. Chem. A* **2003**, *107*, 4578.
(27) Popelier, P. L. A.; Chaudry, U. A.; Smith, P. J. *J. Chem. Soc., Perkin II* **2002**, 1231.
(28) Smith, P. J.; Popelier, P. L. A. *Org. Biomol. Chem.* **2005**, *3*, 3399.
(29) Bader, R. F. W. *Atoms in Molecules. A Quantum Theory*; Oxford University Press: Oxford, U.K., 1990.
(30) Popelier, P. L. A. *Atoms in Molecules. An Introduction.*; Pearson Educ.: Harlow, U.K., 2000.
(31) Dewar, M. J. S.; Zoebisch, E. G.; Healy, E. F.; Stewart, J. J. P. *J. Am. Chem. Soc.* **1985**, *107*, 3902.

(32) Frisch, M. J.; Trucks, G. W.; Schlegel, H. B.; Scuseria, G. E.; Robb, M. A.; Cheeseman, J. R.; Montgomery, J. A., Jr.; Vreven, T.; Kudin, K. N.; Burant, J. C.; Millam, J. M.; Iyengar, S. S.; Tomasi, J.; Barone, V.; Mennucci, B.; Cossi, M.; Scalmani, G.; Rega, N.; Petersson, G. A.; Nakatsuji, H.; Hada, M.; Ehara, M.; Toyota, K.; Fukuda, R.; Hasegawa, J.; Ishida, M.; Nakajima, T.; Honda, Y.; Kitao, O.; Nakai, H.; Klene, M.; Li, X.; Knox, J. E.; Hratchian, H. P.; Cross, J. B.; Bakken, V.; Adamo, C.; Jaramillo, J.; Gomperts, R.; Stratmann, R. E.; Yazyev, O.; Austin, A. J.; Cammi, R.; Pomelli, C.; Ochterski, J. W.; Ayala, P. Y.; Morokuma, K.; Voth, G. A.; Salvador, P.; Dannenberg, J. J.; Zakrzewski, V. G.; Dapprich, S.; Daniels, A. D.; Strain, M. C.; Farkas, O.; Malick, D. K.; Rabuck, A. D.; Raghavachari, K.; Foresman, J. B.; Ortiz, J. V.; Cui, Q.; Baboul, A. G.; Clifford, S.; Cioslowski, J.; Stefanov, B. B.; Liu, G.; Liashenko, A.; Piskorz, P.; Komaromi, I.; Martin, R. L.; Fox, D. J.; Keith, T.; Al-Laham, M. A.; Peng, C. Y.; Nanayakkara, A.; Challacombe, M.; Gill, P. M. W.; Johnson, B.; Chen, W.; Wong, M. W.; Gonzalez, C.; Pople, J. A. *Gaussian 03*; Gaussian, Inc.: Wallingford, CT, 2004.

(33) MORPHY98. A program written by P. L. A. Popelier with a contribution from R. G. A. Bone, UMIST, Manchester, England, EU, 1998.

(34) UMETRICS. SIMCA-P 10.0; info@umetrics.com: www.umetrics.com, Umeå, Sweden, 2002.

(35) Wold, S.; Sjostrom, M.; Eriksson, L. Partial Least Squares Projections to Latent Structures (PLS) in Chemistry. In *Encyclopedia of Computational Chemistry*; Schleyer, P. v. R., Ed.; Wiley: Chichester, G.B., 1998; Vol. 3; p 2006.

(36) Livingstone, D. J. *Data Analysis for Chemists*, 1st ed.; Oxford University Press: Oxford, G.B., 1995.

(37) Ho, M.; Schmider, H.; Edgecombe, K. E.; Smith, V. H. J. *Int. J. Quantum Chem. Quantum Chem. Symp.* **1994**, *28*, 215.

(38) Bader, R. F. W.; Preston, H. J. T. *Intnl. J. Quantum Chem.* **1969**, *3*, 327.

(39) Golbraikh, A.; Tropsha, A. *J. Mol. Graph Model.* **2002**, *20*, 269.

(40) Howard, S. T.; Lamarche, O. *J. Phys. Org. Chem.* **2003**, *16*, 133.

(41) Brinck, T.; Haeberlein, M.; Jonsson, M. *J. Am. Chem. Soc.* **1997**, *119*, 4239.

(42) Dust, J. M.; Arnold, D. R. *J. Am. Chem. Soc.* **1983**, *105*, 1221.

(43) Pratt, D. A.; DiLabio, G. A.; Valgimigli, L.; Pedulli, G. F.; Ingold, K. U. *J. Am. Chem. Soc.* **2002**, *124*, 11085.

(44) Bordwell, F. G.; Cheng, J.-P. *J. Am. Chem. Soc.* **1991**, *113*, 1736.

(45) Litwinienko, G.; Megiel, E.; Wonjnicz, M. *Org. Lett.* **2002**, *4*, 2425.

(46) Fu, Y.; Liu, R.; Liu, L.; Guo, Q.-X. *J. Phys. Org. Chem.* **2004**, *17*, 282.

(47) Bakalbassis, E. G.; Lithoxoidou, A. T.; Vafiadis, A. P. *J. Phys. Chem. A* **2003**, *107*, 8594.

(48) Wright, J. S.; Capenter, D. J.; Mckay, D. J.; Ingold, K. U. *J. Am. Chem. Soc.* **1997**, *119*, 4245.